A varved lake sediment record of the ^{10}Be solar activity proxy for the Lateglacial-Holocene transition

Markus Czymzik[a,*], Florian Adolphi[a], Raimund Muscheler[a], Florian Mekhaldi[a], Celia Martin-Puertas[b], Ala Aldahan[c], Göran Possnert[d], Achim Brauer[b]

[a] Department of Geology, Quaternary Sciences, Lund University, 22362 Lund, Sweden

[b] GFZ-German Research Centre for Geosciences, Section 5.2 Climate Dynamics and Landscape Evolution, 14473 Potsdam, Germany

[c] Department of Geology, United Arab Emirates University, 15551 Al Ain, UAR

[d] Tandem Laboratory, Uppsala University, 75120 Uppsala, Sweden

[*]Corresponding author. Tel.: 0046 46 222 1729. Email address: markus.czymzik@geol.lu.se (M. Czymzik).

Keywords: ^{10}Be, varved lake sediments, solar activity, time-scales

Highlights:

^{10}Be record from varved lake sediments covering the Lateglacial-Holocene transition

New approach quantifies environmental influences on ^{10}Be deposition

Indicates potential of ^{10}Be in varved lake sediments for solar activity reconstruction

Indicates potential of ^{10}Be in varved lake sediments as synchronization tool

Abstract

Solar modulated variations in cosmogenic radionuclide production provide both information on past changes in the activity of the Sun and a global synchronization tool. However, to date the use of cosmogenic radionuclides for these applications is almost exclusively based on ^{10}Be records from ice cores and ^{14}C time-series from tree rings, all including archive-specific limitations. We present the first ^{10}Be record from annually laminated (varved) lake sediments for the Lateglacial-Holocene transition from Meerfelder Maar. We quantify environmental influences on the catchment and, consequently, ^{10}Be deposition using a new approach based on regression analyses between our ^{10}Be record and environmental proxy time-series from the same archive. Our analyses suggest that environmental influences contribute to up to 37 % of the variability in our ^{10}Be record, but cannot be the main explanation for major ^{10}Be excursions. Corrected for these environmental influences, our ^{10}Be record is interpreted to dominantly reflect changes in solar modulated cosmogenic radionuclide production. The preservation of a solar production signal in ^{10}Be from varved lake sediments highlights the largely unexplored potential of these archives for solar activity reconstruction, as global synchronization tool and, thus, for more robust paleoclimate studies.

1. Introduction

Changes in solar activity have been suggested to influence past and modern climates (Gray et al., 2010). An accurate knowledge of changes in the activity of the Sun is crucial for understanding solar influences on climate (Gray et al., 2010). Before satellite measurements of solar irradiation and the observation of sunspots, cosmogenic radionuclides like ^{10}Be in polar ice cores and ^{14}C in tree rings provide key information on changes in solar activity (Beer et al., 1990; Muscheler et al., 2007; Vonmoos et al., 2006). ^{10}Be is produced in the upper atmosphere (about ⅔ in the stratosphere and ⅓ in the troposphere) as by-product of cascades of nuclear reactions induced by incident high-energy galactic cosmic rays (Lal and Peters, 1967). The flux of these galactic cosmic rays towards the atmosphere is modulated by solar activity variations through varying heliomagnetic shielding (Lal and Peters, 1967). During periods of higher solar activity and stronger heliomagnetic shielding, less galactic cosmic rays reach the atmosphere and less ^{10}Be is produced. Further ^{10}Be production rate changes introduced by the varying geomagnetic field strength become most likely significant only on >500-year time-scales (Snowball and Muscheler, 2007).

In addition to the atmospheric production, available cosmogenic radionuclide records are to a varying degree affected by archive-specific so-called system effects: Changing exchange rates between Earth's carbon reservoirs add non-production variations to the atmospheric ^{14}C record (Muscheler et al., 2004). Theoretically, this effect can be accounted for by using a carbon cycle model to calculate the atmospheric ^{14}C production. However, past exchanges between carbon reservoirs are difficult to quantify, particularly in times of abrupt climate changes (Köhler et al., 2006). While ^{10}Be is in comparison to ^{14}C geochemically more stable and thus in principle a more direct indicator of the production rate, inhomogeneous tropospheric mixing and precipitation during the short about 1 to 2-year atmospheric residence time (Raisbeck et al., 1981) cause spatially varying ^{10}Be deposition patterns (Heikkilä et al., 2013; Pedro et al., 2012). Further uncertainties in available ice core ^{10}Be records arise from the assumed depositional mode. In case of wet deposition ^{10}Be concentrations, and in case of dry deposition ^{10}Be fluxes would best reflect the atmospheric production signal (Alley et al., 1995; Delaygue and Bard, 2011). However, no single depositional mode correctly reflects reality and the dominant mode of deposition can change over time (Alley et al., 1995). Exploring the potential of ^{10}Be in new archives like varved lake sediments offers a complementary approach for tracking the atmospheric ^{10}Be production signal and, thereby, could improve our knowledge on past changes in solar activity.

To date, the potential of ^{10}Be in varved lake sediments is largely unexplored. Chronologies based on varve counting enable the establishment of ^{10}Be records at a chronological precision that is comparable to that for ice cores or tree rings. First calibration studies of annually resolved ^{10}Be time-series from three varved lake sediment archives yielded a correlation between changes in ^{10}Be and solar activity during the 11-year solar 'Schwabe' cycle (Berggren et al., 2010; Czymzik et al., 2015). However, further correspondences with proxy time-series also suggest that environmental factors like e.g. varying organic matter contents and sediment redeposition may influence ^{10}Be deposition in these lakes (Czymzik et al., 2015). Therefore, more detailed investigations are needed to improve the use of ^{10}Be in varved lake sediments as indicator of the atmospheric production rate and, thereby, solar activity. In addition, detecting the common atmospheric radionuclide production signal in varved lake sediments provides the opportunity for continuous climate-independent synchronizations to cosmogenic radionuclide records worldwide. Such a synchronization could e.g. contribute to the discussion on the unresolved rapid chronological shift between the GICC05 ice core and ^{14}C time-scales around the Younger Dryas (Adolphi and Muscheler, 2016; Muscheler et al., 2014).

The varved Meerfelder Maar (MFM) lake sediment record is a well-established paleoenvironmental archive, particularly for the Lateglacial-Holocene transition (Brauer et al., 2008, 1999; Engels et al., 2015; Lane et al., 2015; Lücke and Brauer, 2004; Rach et al., 2014). Increased ^{10}Be accumulation rates coinciding with an interval of thicker varves enabled the linkage of a grand solar minimum about 2800 years ago with a synchronous change in regional atmospheric circulation in times of moderate climate variations (Martin-Puertas et al., 2012b). Here, we present the first lake sediment record of ^{10}Be concentrations ($^{10}Be_{con}$) at ~20-year resolution covering the Lateglacial-Holocene transition (11310 to 13130 varve a BP; i.e. before AD 1950) from MFM. A novel methodological approach based on complementary environmental proxy time-series from the same archive allows us to systematically investigate the depositional mechanisms and, thereby, track solar induced changes in the atmospheric ^{10}Be production rate. Spanning the early Holocene, Younger Dryas and late Allerød, our record enables us to test the robustness of our results on ^{10}Be deposition in MFM sediments under varying sedimentary regimes and climatic boundary conditions.

2. Study site

Meerfelder Maar is situated within the Westeifel Volcanic field (50°6'N, 6°45'E), at an elevation of 334 m a.s.l. (Fig. 1). The contemporary lake has a depth of 18 m and a surface area of 0.25 km^2, covering about ⅓ of the about 150 m deep crater surface (Fig. 1). Meerfelder Maar sediments are continuously varved between ~1500 and 14230 varve a BP (Brauer et al., 2000). Varves during the Holocene comprise couples of diatom and detrital sub-layers. Within the Lateglacial, snowmelt varves (late Younger Dryas), clastic-organic varves (early Younger Dryas) and Fe-rich siderite varves (late Allerød) have been formed (Brauer et al., 1999; Martin-Puertas et al., 2012a). Varve formation in MFM is sensitive to North Atlantic climate variations (Brauer et al., 2008; Martin-Puertas et al., 2012b)

3. Methods

3.1. Sediment sub-sampling

Bulk sediment samples for ^{10}Be measurements were extracted from composite profile MFM09 (Lane et al., 2015; Martin-Puertas et al., 2012a) at about 20-year resolution, excluding the Laacher See Tephra. Upper and lower sample boundaries were determined using macroscopic varved dated marker layers (Brauer et al., 2000; Lane et al., 2015).

3.2. ^{10}Be extraction and AMS measurements

After drying and homogenizing, 0.5 mg ^{9}Be carrier was added to 0.5 g sediment material and Be leached overnight with 7.5 ml 8 M HCl at 60°C. The solution was subsequently filtered to remove the undissolved fractions. Further addition of NH_3, EDTA and H_2SO_4 induced the precipitation of metal hydroxides, other metals and silicates which were again separated from the solution by filtering (Berggren et al., 2010). The remaining solution was then passed through ion exchange columns (Bio-Rad Polyprep Prefilled Chromatography Columns, 100-200 mesh, hydrogen form) in which Be was retained (Berggren et al., 2010). Be was extracted from the columns through the addition of 7 ml 4 M HCl, and $Be(OH)_2$ precipitated in a warm water bath using NH_3 (25 %, Suprapur). The samples were washed and dehydrated three times with warm 2 % NH_4NO_3 and oxidized to BeO by heating to 600°C. Finally, the samples were mixed with Nb and pressed into sample holders. AMS measurements of BeO were performed at the Uppsala Tandem Laboratory using the reference standard NIST SRM 4325 ($^{10}Be/^{9}Be = 2.68*10^{-11}$) (Berggren et al., 2010).

3.3. Environmental proxy time-series

Geochemical, total organic carbon (TOC) and sediment accumulation rate (SAR) datasets at the about 20-year resolution of the ^{10}Be data were constructed from available higher resolution time-series. The element composition was measured on cleaned sediment core halves at 200 µm resolution using an ITRAX X-ray fluorescence (μ-XRF) scanner (Martin-Puertas et al., 2012a). Measured element intensities were centered log-ratio (clr) transformed to minimize the effects of varying sediment properties (Weltje and Tjallingii, 2008). TOC contents of a continuous series of sediment samples were determined from 4 mg decalcified sample aliquots in Ag-capsules using an EA3000-CHNS elemental analyzer. The SAR (g cm^{-2} $year^{-1}$) is the product of varve thickness (cm $year^{-1}$) and dry density (g cm^{-3}), reflecting a mixture of changes in the deposited sediment volume and composition (Zolitschka, 1998). Microscopic varve thickness measurements were performed on series of overlapping petrographic thin-sections (Brauer et al., 2000; Lane et al., 2015; Martin-Puertas et al., 2012a). Dry density was determined by weighing freeze-dried 1 cm^3 sediment samples.

3.4. Chronology

All investigated time-series are on the MFM2015 time-scale, established by means of varve counting and fixed to the absolute time-scale using tephrochronology and radiocarbon dating (for details see: Brauer et al., 2000, 1999; Lane et al., 2015; Martin-Puertas et al., 2012a). The Vedde Ash in the MFM2015 (12140 ± 40 varve a BP) (Lane et al., 2013) and GICC05 time-scales (12121 ± 114 a BP) (Rasmussen et al., 2006), located about midway through the investigated MFM sediment interval, provides an independent tie-point for a comparison of the MFM ^{10}Be record to those from the GRIP and GISP2 ice cores.

3.5. Statistical significance

Statistical significances of correlations between the $^{10}Be_{con}$ record and environmental proxy time-series were assessed using a non-parametric random-phase test (Ebisuzaki, 1997). The test takes into account the effects of autocorrelation present in the time-series (Ebisuzaki, 1997). First, 10000 versions of the $^{10}Be_{con}$ record were computed that have an identical frequency spectrum as the original record, but randomly differ in the phase of each frequency. The statistical significances of the correlations between the ^{10}Be record and the environmental proxy time-series were then determined by replacing the original $^{10}Be_{con}$ record with its phase shifted surrogates and calculating the probability distribution of the correlations that occur by chance.

4. Results

$^{10}Be_{con}$ were measured in 96 sediment samples from a 158 cm long section (725 to 882 cm composite depth) of composite profile MFM09 (Lane et al., 2015; Martin-Puertas et al., 2012a) (Fig. 2). Mean $^{10}Be_{con}$ is 2.7*10^8 atoms g^{-1}. $^{10}Be_{con}$ vary distinctly between 2 and 4.7*10^8 atoms g^{-1} (mean 3*10^8 atoms g^{-1}) from 820 to 882 cm composite depth and depict smaller variability between 1.8 and 3.3*10^8 atoms g^{-1} (mean 2.5*10^8 atoms g^{-1}) from 725 to 817 cm composite depth (Fig. 2). Mean AMS measuring uncertainty is 0.1*10^8 atoms g^{-1}. A series of 6 MFM sediment samples yielded $^{10}Be_{con}$ up to 45.9*10^8 atoms g^{-1}, distinguished from the remaining record by their exceptionally high ^{10}Be concentrations (up to a factor of 17 higher than the mean of the remaining $^{10}Be_{con}$ record). Since (i) we did not observe coinciding distinct changes in sediment accumulation or composition and, (ii) more importantly, these anomalous high values were not replicated by ^{10}Be measurements in sediment samples from the same core position, these six data points were treated as measurement outliers and excluded from the analyses. Due to the 1.387 ± 0.012 Ma long half-life of ^{10}Be (Korschinek et al., 2010) the effect of radioactive decay is negligible in our about 2000-year long ^{10}Be record from the Lateglacial-Holocene transition.

5. Discussion

5.1. Environmental effects on $^{10}Be_{con}$ deposition

Regional environmental variations during the Lateglacial-Holocene transition modify catchment processes and might, therefore, bias the atmospheric ^{10}Be production signal in lake sediment archives. Comparing the MFM $^{10}Be_{con}$ record to sedimentological and geochemical proxy time-series from the same archive allows us to evaluate these effects.

Changing sediment accumulation rates (SAR) might influence $^{10}Be_{con}$ in MFM sediments by diluting them more (higher SAR) or less (lower SAR) (Berggren et al., 2010). This is potentially reflected by a significant negative correlation between $^{10}Be_{con}$ and SAR ($r=-0.39$, $p<0.01$) (Figs. 2 and 3). However, despite this correlation, major changes in SAR (e.g. around 750, 800 and 851 cm composite depth) are not reflected by the MFM $^{10}Be_{con}$ record (Fig. 2).

Relationships with $^{10}Be_{con}$ are further noticeable for the element Ti and the Si/Ti ratio, reflecting main sediment components in MFM during the Lateglacial-Holocene transition (Brauer et al., 1999) (Figs. 2 and 3). Ti is indicative of detrital material transported from the catchment into the lake (Martin-Puertas et al., 2012a) and exhibits a significant negative correlation with $^{10}Be_{con}$ ($r=-0.39$, $p<0.01$) (Fig. 2). However, neither major rises (e.g. at 802 cm composite depth) nor drops in Ti (e.g. at 748 cm composite depth) are paralleled by major shifts in the $^{10}Be_{con}$ record (Fig. 2). The Si/Ti ratio is interpreted as an indicator of diatom abundances since Si in MFM sediments represents both detrital input and diatom deposition, while Ti is related to detrital influx only (Martin-Puertas et al., 2012a) (Fig. 2). Like Ti, the Si/Ti ratio is significantly correlated with $^{10}Be_{con}$ ($r=0.17$, $p=0.07$), but major shifts in this proxy (e.g. around 728 and 802 cm composite depth) do not correspond to major changes in $^{10}Be_{con}$ (Fig. 2).

Further uncertainties in ^{10}Be production time-series from lake sediments could be caused through the preferential binding of ^{10}Be to a particular sediment fraction. It was suggested that Fe and organic matter are favorable carriers of ^{10}Be (Mann et al., 2012; Willenbring and von Blanckenburg, 2010). High Fe values from 857 to 877 cm composite depth reflect the deposition of siderite varves in MFM, indicative of anoxic bottom water conditions (Fig. 2) (Brauer et al., 2008). $^{10}Be_{con}$ and Fe exhibit a significant correlation in the investigated sediments ($r=0.32$, $p<0.01$) (Figs. 2 and 3). However, even though the major drop in Fe at 855 cm composite depth coincides with a distinct decrease in $^{10}Be_{con}$, other shifts in Fe (e.g. at 740, 760 and 832 cm composite depth) are not reflected in the $^{10}Be_{con}$ record (Fig. 2). These results suggest that the amplitudes of the variations in our $^{10}Be_{con}$ record caused by a potential preferential binding to Fe are likely small. One possible reason for this small influence might be that iron cycling in lakes occurs predominantly at the water-sediment interface (Davison, 1993), while ^{10}Be scavenging likely takes place throughout the entire water column.

Positive correlations point to a preferential binding of ^{10}Be to organic material in previously measured annually resolved ^{10}Be time-series from recent varved sediments of two central European lakes (Czymzik et al., 2015). While mean TOC concentrations in these two lake sediments are about 10 %, they are generally lower in the investigated MFM sediments (mean 4.5 %), with only one short peak reaching about 10 % at 855 cm composite depth (Fig. 2). Nevertheless, $^{10}Be_{con}$ and TOC are significantly correlated in the investigated MFM sediment record (r=0.44, p<0.01) (Fig. 2). However, except for the mentioned peak around 855 cm composite depth, other major shifts in TOC (e.g. at 748 and 798 cm composite depth) do not correspond to distinct changes in the $^{10}Be_{con}$ record (Fig. 2). Therefore, potential effects of a preferential binding to TOC likely introduce minor variations and do not obscure major excursions in our $^{10}Be_{con}$ record. A reason for this weak linkage to $^{10}Be_{con}$ might be the low TOC concentrations in the investigated MFM sediment interval (Fig. 2). Small effects of a preferential binding of ^{10}Be to TOC and Fe are in agreement with a review study concluding that no single constituent dominates the distribution of ^{10}Be in soils (Graly et al., 2010).

Mean $^{10}Be_{con}$ are about 10 % higher during the early Holocene ($2.8*10^8$ atoms g^{-1}) and about 20 % higher during the late Allerød ($3*10^8$ atoms g^{-1}), compared to the Younger Dryas ($2.5*10^8$ atoms g^{-1}) (Fig. 2). Varying mean $^{10}Be_{con}$ during the three climate periods could be explained by changes in tropospheric mixing and precipitation (Heikkilä et al., 2013) and catchment processes (Czymzik et al., 2015), but also by different atmospheric ^{10}Be production rates, all potentially modifying ^{10}Be deposition at MFM. However, mean $^{10}Be_{con}$ changes during these three climate periods do not exceed 20 %, compared to the about 90 % variations during major $^{10}Be_{con}$ excursions (Fig. 2).

To summarize, comparing the MFM $^{10}Be_{con}$ record to proxy time-series from the same archive suggests that environmental influences on the catchment cannot be the main explanation for major $^{10}Be_{con}$ excursions in the investigated MFM sediments (e.g. around 750, 820, 855 and 875 cm composite depth) (Fig. 2). Nevertheless, significant correlations between $^{10}Be_{con}$ and SAR, Ti, Si/Ti ratio, TOC and Fe point to influences of varying catchment conditions on $^{10}Be_{con}$ deposition in our archive (Figs. 2 and 3). In the following section we aim at quantifying and correcting for these influences on $^{10}Be_{con}$ deposition in order to extract a regional atmospheric input signal.

5.2. Regional atmospheric ^{10}Be input

In an attempt to extract a regional atmospheric input signal ($^{10}Be_{con}$ corrected for the effects of environmental influences on catchment conditions and ^{10}Be deposition), a two-step procedure was applied to the MFM $^{10}Be_{con}$ record. First, simple linear regressions were calculated between the MFM $^{10}Be_{con}$ record and the significantly correlated proxy time-series SAR, Ti, Si/Ti ratio, TOC and Fe separately, to determine the likely environmental bias ($^{10}Be_{bias}$). Second, the resulting $^{10}Be_{bias}$ time-series were subtracted from the original MFM $^{10}Be_{con}$ record to approximate the regional atmospheric ^{10}Be input ($^{10}Be_{atmosphere}$) (Fig. 4a). The equations are as follows:

(1) $^{10}Be_{bias} = a + x * proxy$

(2) $^{10}Be_{atmosphere} = (^{10}Be_{con} - {}^{10}Be_{bias} + mean\ (^{10}Be_{con})) / mean(^{10}Be_{con})$

For evaluating the possibly largest environmental bias on ^{10}Be deposition, we further calculated a $^{10}Be_{atmosphere}$ time-series performing a multiple regression analysis between our $^{10}Be_{con}$ record and all proxy time-series with a significant correlation (Fig. 4a). The final $^{10}Be_{atmosphere}$ curve includes only corrections from proxy time-series with a significant contribution (>90 % level: Si/Ti ratio, TOC) to the final multiple regression (Table 1).

All six calculated $^{10}Be_{atmosphere}$ time-series depict similar multi-decadal variability and trends, compared to the original MFM $^{10}Be_{con}$ record (Fig. 4a). Changing environmental conditions ($^{10}Be_{bias}$) explain between 8 and 29 % (mean 18 %) of the variance when the $^{10}Be_{con}$ record is corrected using the individual SAR, Ti, Si/Ti ratio, TOC and Fe time-series (Table 1). Corrected using all significantly correlated proxy time-series, $^{10}Be_{bias}$ explains 37 % of the variations in the $^{10}Be_{con}$ record (Fig. 4a, Table 1). The amplitude of the older part of the $^{10}Be_{con}$ peak from 12670 to 12770 varve a BP is broadly unchanged when $^{10}Be_{atmosphere}$ is calculated using SAR, Ti, Si/Ti ratio and Fe, but reduced by about 30 % when $^{10}Be_{atmosphere}$ is calculated using TOC and all significantly correlated proxy time-series (Fig. 4a).

To test the robustness of these corrections, we calculated the six $^{10}Be_{atmosphere}$ time-series separately for the early Holocene, Younger Dryas and late Allerød (Fig. 4b). The calculated $^{10}Be_{atmosphere}$ time-series for the individual climate periods resemble those for the complete record (Fig. 4). This test illustrates that the corrections of the $^{10}Be_{con}$ record are not influenced by varying environmental conditions and sedimentary regimes connected to the three climate periods.

To conclude, in our analyses environmental influences on catchment conditions account for up to 37 % of the variability in the MFM $^{10}Be_{con}$ record. Corrected for these influences, the resulting $^{10}Be_{atmosphere}$ time-series likely reflect a regional atmospheric input signal. In the following section we will discuss connections between the MFM $^{10}Be_{atmosphere}$ time-series and changes in solar activity inferred from other cosmogenic radionuclide records as well as the effects of inhomogeneous tropospheric mixing and precipitation, which are presumably not recorded by the MFM proxy time-series.

5.3. Solar modulated ^{10}Be production

For deciphering solar modulated changes in ^{10}Be production, we compare a composite (to reduce noise) of the six MFM $^{10}Be_{atmosphere}$ time-series to ^{10}Be fluxes from the GRIP (Adolphi et al., 2014) and GISP2 ice cores (Finkel and Nishiizumi, 1997) and ^{14}C production rates derived from tree rings (Muscheler et al., 2014) (Fig. 5). A 500-year high-pass filter was applied to the time-series to minimize the effects of the varying geomagnetic field on cosmogenic radionuclide production (Snowball and Muscheler, 2007). This filter also reduces system effects that are potentially present in the ^{10}Be and ^{14}C records (Adolphi and Muscheler, 2016). The shared variance of the radionuclide records can be considered as an indicator of the solar modulated cosmogenic radionuclide production rate (Muscheler et al., 2007). Maximum differences between the individual $^{10}Be_{atmosphere}$ time-series at each point were used as uncertainty ranges (Fig. 5). In addition, bandpass filtering was applied to the cosmogenic radionuclide records to focus on the frequency ranges of the solar Gleissberg (frequencies between 1/75 and 1/100 years^{-1}) and De Vries (frequencies between 1/180 and 1/230 years^{-1}) cycles (Fig. 6). The Vedde Ash dated to 12140 ± 40 varve a BP in the MFM2015 and 12121 ± 114 a BP in the GICC05 time-scale (Lane et al., 2013; Rasmussen et al., 2006) indicates no age-scale difference between the MFM and GRIP/GISP2 ice core records, within the dating uncertainties (Fig. 5).

Most distinctive features of the MFM $^{10}Be_{atmosphere}$ composite are three peaks centered at 12400, 12750 and 13050 varve a BP and a minimum around 11650 varve a BP (Fig. 5). All these features are also visible in the ^{14}C production rate and GRIP and GISP2 ^{10}Be flux records suggesting that they are related to common solar modulated radionuclide production changes (Fig. 5). Differences between the ^{10}Be records from MFM and the ice cores might be explained by inhomogeneous tropospheric mixing and precipitation causing differing ^{10}Be deposition patterns at the sites of MFM and the ice cores (McHargue and Damon, 1991). Differences between the MFM $^{10}Be_{con}$ record and the ^{14}C production rate could be further due to uncorrected carbon cycle influences on the ^{14}C production record (McHargue and Damon, 1991; Siegenthaler et al., 1980). After the production, ^{14}C oxidizes to $^{14}CO_2$ and enters the global carbon cycle while ^{10}Be attaches to aerosols (McHargue and Damon, 1991; Siegenthaler et al., 1980). Temporal offsets between the MFM and ice core ^{10}Be records might be explained by time-scale differences within the dating uncertainties (Fig. 5).

In the frequency range of the solar Gleissberg cycle, the MFM $^{10}Be_{atmosphere}$ composite reveals a good agreement with ^{10}Be fluxes in the GRIP ice core and ^{14}C production rates (Fig. 6). The different phase relationship around 12800 a BP might be caused by inhomogeneous tropospheric mixing and precipitation, uncorrected carbon cycle influences, time-scale differences within the dating uncertainties (see the paragraph above for details) and/or a single data point with high/low values that can lead to the inclusion or exclusion of a cycle in the narrowly filtered time-series (Fig. 6). The about 50-year resolution of the GISP2 ^{10}Be flux record inhibits investigating variations in the Gleissberg cycle frequency range.

All four cosmogenic radionuclide records reveal notable variability within the frequency range of the solar De Vries cycle (Fig. 6). However, while these variations in the $^{10}Be_{atmosphere}$ composite are in-phase with those in the GRIP ^{10}Be flux and ^{14}C production rate records from 11310 to about 12500 a BP, they reveal different relationships and amplitudes from about 12520 to 13310 a BP (Fig. 6). Again, the most likely explanation for these differences might be inhomogeneous tropospheric mixing and precipitation, uncorrected carbon cycle influences, time-scale differences within dating uncertainties (see the paragraph above for details) and single outlying data points. The same reasons could explain the phase shift between the MFM $^{10}Be_{atmosphere}$ composite and the GISP2 ^{10}Be flux record (Fig. 6).

To summarize, similarities with the reconstructed ^{14}C production rate and ^{10}Be fluxes in the GRIP and GISP2 ice cores suggest the preservation of the solar production signal in the MFM $^{10}Be_{atmosphere}$ composite. Remaining differences between the MFM $^{10}Be_{atmosphere}$ composite and the other cosmogenic radionuclide time-series point to inhomogeneous tropospheric mixing and precipitation, uncorrected carbon cycle influences and/or time-scale differences within the dating uncertainties.

5.4. Mechanisms of ^{10}Be deposition

The preservation of the solar modulated production signal in MFM $^{10}Be_{atmosphere}$ allows us to draw conclusions about to the depositional mechanisms: (i) Increased sediment flux through the water column tends to increase ^{10}Be scavenging and, thereby, does not distinctly influence ^{10}Be concentrations in the sediments (major excursions in SAR are not mirrored by $^{10}Be_{con}$ changes of opposite sign (Fig. 2) and ^{10}Be availability does not seem to be a limiting factor in our study) and (ii) higher ^{10}Be concentrations in the lake water increase the amount of ^{10}Be atoms deposited by each sediment particle. In combination, these two effects are comparable to the proposed ^{10}Be wet deposition in ice cores (Alley et al., 1995) and supported by sediment trap studies on ^{7}Be and ^{10}Be deposition in Lakes Constance and Zurich (Schuler et al., 1991; Vogler et al., 1996). Both sediment trap studies suggest that Be deposition in the lakes is controlled by the particle flux through the water column and atmospheric ^{10}Be input (Schuler et al., 1991; Vogler et al., 1996). Results on ^{7}Be can be transferred to those from ^{10}Be since both isotopes behave chemically identical (Aldahan et al., 1999).

On multi-decadal to centennial scales, ^{10}Be fluxes in the GRIP and GISP2 ice cores during the Holocene vary by about 50 % (Muscheler and Heikkilä, 2011). These variations are in agreement with estimates of solar induced ^{10}Be production rate changes on such time-scales (Masarik and Beer, 1999; Muscheler and Heikkilä, 2011). However, $^{10}Be_{con}$ in the investigated MFM sediments shows up to 90 % variability (Fig. 2). Therefore, ^{10}Be flux from the catchment into the lake by surface runoff is likely to contribute to the larger variability in the MFM $^{10}Be_{con}$ record.

6. Conclusions

We present the first ^{10}Be record from varved lake sediments for the Lateglacial-Holocene transition from Meerfelder Maar. We attempt to quantify regional environmental influences on catchment conditions and ^{10}Be deposition based on regression analyses between our ^{10}Be record and proxy time-series from the same archive. Regional environmental influences contribute to up to 37 % of the variability in our ^{10}Be record, but cannot explain major ^{10}Be excursions. Corrected for environmental influences, our ^{10}Be record is interpreted to dominantly reflect changes in solar modulated cosmogenic radionuclide production. The preservation of the solar production signal indicates the large potential of ^{10}Be in varved lake sediments for solar activity reconstruction and as global synchronization tool. However, our results also indicate the importance of a mechanistic understanding of, partly site-specific, environmental effects on ^{10}Be deposition in lake sediment archives. Therefore, more studies of ^{10}Be in varved sediments from lakes with different lake/catchment characteristics can help to further improve the application of this proxy as indicator of the atmospheric cosmogenic radionuclide production rate.

Acknowledgements

MC was funded by a German Science Foundation postdoc grant (DFG grant CZ 227/1-1) and the Swedish Research Council (VR grant to RM: Dnr: 2013-8421). Further financial support was provided through a travel grant from the EU COST action ES0907 INTIMATE, an endowment from the Royal Physiographic Society in Lund and a Linnaeus grant to Lund University (LUCCI). We would like to thank Inger Påhlsson for the extraction of ^{10}Be from sediment samples and Oliver Rach for measuring TOC contents. ^{10}Be data are available at the PANGAEA data library. We thank two anonymous reviewers for their constructive comments.

References

Adolphi, F., Muscheler, R., 2016. Synchronizing the Greenland ice core and radiocarbon timescales over the Holocene - Bayesian wiggle-matching of cosmogenic radionuclide records. Clim. Past 12, 15–30. doi:10.5194/cp-12-15-2016

Adolphi, F., Muscheler, R., Svensson, A., Aldahan, A., Possnert, G., Beer, J., Sjolte, J., Björck, S., Matthes, K., Thiéblemont, R., 2014. Persistent link between solar activity and Greenland climate during the Last Glacial Maximum. Nat. Geosci. 7, 662–666. doi:10.1038/ngeo2225

Aldahan, A., Ye, H.P., Possnert, G., 1999. Distribution of beryllium between solution and minerals (biotite and albite) under atmospheric conditions and variable pH. Chem. Geol. 156, 209–229. doi:10.1016/s0009-2541(98)00186-7

Alley, R.B., Finkel, R.C., Nishiizumi, K., Anandakrishnan, S., Shuman, C.A., Mershon, G., Zielinski, G.A., Mayewski, P.A., 1995. Changes in continental and sea-salt atmospheric loadings in central Greenland during the most recent deglaciation: model-based estimates. J. Glaciol. 41, 503–514.

Beer, J., Blinov, B., Bonani, G., Finkel, R.C., Hofmann, H.J., Lehmann, B., Oeschger, H., Sigg, A., Schwander, J., Staffelbach, T., Stauffer, B., Suter, M., Wölfli, W., 1990. Use of ^{10}Be in polar ice to trace the 11-year cycle of solar activity. Nature 347, 164–166.

Berggren, A.M., Aldahan, A., Possnert, G., Haltia-Hovi, E., Saarinen, T., 2010. ^{10}Be and solar activity cycles in varved lake sediments, AD 1900-2006. J. Paleolimnol. 44, 559–569. doi:10.1007/s10933-010-9437-1

Brauer, A., Endres, C., Günter, C., Litt, T., Stebich, M., Negendank, J.F.W., 1999. High resolution sediment and vegetation responses to Younger Dryas climate change in varved lake sediments from Meerfelder Maar, Germany. Quat. Sci. Rev. 18, 321–329. doi:10.1016/S0277-3791(98)00084-5

Brauer, A., Endres, C., Zolitschka, B., Negendank, J.F.W., 2000. AMS radiocarbon and varve chronology from the annually laminated sediment record of Lake Meerfelder Maar, Germany. Radiocarbon 42, 355–368. doi:10.2458/azu_js_rc.42.3828

Brauer, A., Haug, G.H., Dulski, P., Sigman, D.M., Negendank, J.F.W., 2008. An abrupt wind shift in western Europe at the onset of the Younger Dryas cold period. Nat. Geosci. 1, 520–523. doi:10.1038/ngeo263

Czymzik, M., Muscheler, R., Brauer, A., Adolphi, F., Ott, F., Kienel, U., Dräger, N., Słowiński, M., Aldahan, A., Possnert, G., 2015. Solar cycles and depositional processes in annual ^{10}Be from two varved lake sediment records. Earth Planet. Sci. Lett. 428, 44–51. doi:10.1016/j.epsl.2015.07.037

Davison, W., 1993. Iron and manganese in lakes. Earth-Science Rev. 34, 119–163. doi:10.2307/41226456

Delaygue, G., Bard, E., 2011. An Antarctic view of Beryllium-10 and solar activity for the past millennium. Clim. Dyn. 36, 2201–2218. doi:10.1007/s00382-010-0795-1

Ebisuzaki, W., 1997. A method to estimate the statistical significance of a correlation when the data are serially correlated. J. Clim. 10, 2147–2153. doi:10.1175/1520-0442(1997)010<2147:AMTETS>2.0.CO;2

Engels, S., van Geel, B., Buddelmeijer, N., Brauer, A., 2015. High-resolution palynological evidence for vegetation response to the Laacher See eruption from the varved record of Meerfelder Maar (Germany) and other central European records. Rev. Palaeobot. Palynol. 221, 160–170. doi:10.1016/j.revpalbo.2015.06.010

Finkel, R.C., Nishiizumi, K., 1997. Beryllium 10 concentrations in the Greenland Ice Sheet Project 2 ice core from 3-40 ka. J. Geophys. Res. 102, 26699–26706.

Graly, J.A., Bierman, P.R., Reusser, L.J., Pavich, M.J., 2010. Meteoric ^{10}Be in soil profiles - A global meta-analysis. Geochim. Cosmochim. Acta 74, 6814–6829. doi:10.1016/j.gca.2010.08.036

Gray, L.J., Beer, J., Geller, M., Haigh, J.D., Lockwood, M., Matthes, K., Cubasch, U., Fleitmann, D., Harrison, G., Hood, L., Luterbacher, J., Meehl, G.A., Shindell, D., van Geel, B., White, W., 2010. Solar influences on climate. Rev. Geophys. 48, RG4001. doi:10.1029/2009RG000282

Heikkilä, U., Beer, J., Abreu, J.A., Steinhilber, F., 2013. On the atmospheric transport and deposition of the cosmogenic radionuclides (^{10}Be): A review. Space Sci. Rev. 176, 321–332. doi:10.1007/s11214-011-9838-0

Köhler, P., Muscheler, R., Fischer, H., 2006. A model-based interpretation of low-frequency changes in the carbon cycle during the last 120,000 years and its implications for the reconstruction of atmospheric Δ^{14}C. Geochemistry, Geophys. Geosystems 7, Q11N06. doi:10.1029/2005GC001228

Korschinek, G., Bergmaier, A., Faestermann, T., Gerstmann, U.C., Knie, K., Rugel, G., Wallner, A., Dillmann, I., Dollinger, G., von Gostomski, C.L., Kossert, K., Maiti, M., Poutivtsev, M., Remmert, A., 2010. A new value for the half-life of ^{10}Be by Heavy-Ion Elastic Recoil Detection and liquid scintillation counting. Nucl. Instruments Methods Phys. Res. Sect. B Beam Interact. with Mater. Atoms 268, 187–191. doi:10.1016/j.nimb.2009.09.020

Lal, D., Peters, B., 1967. Cosmic ray produced radioactivity on the Earth, in: Flügge, S. (Ed.), Handbuch Der Physik. Springer, Berlin, pp. 551–612. doi:10.1007/978-3-642-46079-1

Lane, C.S., Brauer, A., Blockley, S.P.E., Dulski, P., 2013. Volcanic ash reveals time-transgressive abrupt climate change during the Younger Dryas. Geology 41, 1251–1254. doi:10.1130/G34867.1

Lane, C.S., Brauer, A., Martin-Puertas, C., Blockley, S.P.E., Smith, V.C., Tomlinson, E.L., 2015. The Late Quaternary tephrostratigraphy of annually laminated sediments from Meerfelder Maar, Germany. Quat. Sci. Rev. 122, 192–206. doi:10.1016/j.quascirev.2015.05.025

Lücke, A., Brauer, A., 2004. Biogeochemical and micro-facial fingerprints of ecosystem response to rapid Late Glacial climatic changes in varved sediments of Meerfelder Maar (Germany). Palaeogeogr. Palaeoclimatol. Palaeoecol. 211, 139–155. doi:10.1016/j.palaeo.2004.05.006

Mann, M., Beer, J., Steinhilber, F., Christl, M., 2012. ^{10}Be in lacustrine sediments - A record of solar activity? J. Atmos. Solar-Terrestrial Phys. 80, 92–99. doi:10.1016/j.jastp.2012.03.011

Martin-Puertas, C., Brauer, A., Dulski, P., Brademann, B., 2012a. Testing climate-proxy stationarity throughout the Holocene: An example from the varved sediments of Lake Meerfelder Maar (Germany). Quat. Sci. Rev. 58, 56–65. doi:10.1016/j.quascirev.2012.10.023

Martin-Puertas, C., Matthes, K., Brauer, A., Muscheler, R., Hansen, F., Petrick, C., Aldahan, A., Possnert, G., van Geel, B., 2012b. Regional atmospheric circulation shifts induced by a grand solar minimum. Nat. Geosci. 5, 397–401. doi:10.1038/ngeo1460

Masarik, J., Beer, J., 1999. Simulation of particle fluxes and cosmogenic nuclide production in the Earth's atmosphere. J. Geophys. Res. 104, 12099–12111.

McHargue, L.R., Damon, P.E., 1991. The global Beryllium 10 cycle. Rev. Geophys. 29, 141–158.

Muscheler, R., Adolphi, F., Knudsen, M.F., 2014. Assessing the differences between the IntCal and Greenland ice-core time scales for the last 14,000 years via the common cosmogenic radionuclide variations. Quat. Sci. Rev. 106, 81–87. doi:10.1016/j.quascirev.2014.08.017

Muscheler, R., Beer, J., Wagner, G., Laj, C., Kissel, C., Raisbeck, G.M., Yiou, F., Kubik, P.W., 2004. Changes in the carbon cycle during the last deglaciation as indicated by the comparison of ^{10}Be and ^{14}C records. Earth Planet. Sci. Lett. 219, 325–340. doi:10.1016/S0012-821X(03)00722-2

Muscheler, R., Heikkilä, U., 2011. Constraints on long-term changes in solar activity from the range of variability of cosmogenic radionuclide records. Astrophys. Sp. Sci. Trans. 7, 355–364. doi:10.5194/astra-7-355-2011

Muscheler, R., Joos, F., Beer, J., Müller, S.A., Vonmoos, M., Snowball, I., 2007. Solar activity during the last 1000 yr inferred from radionuclide records. Quat. Sci. Rev. 26, 82–97. doi:10.1016/j.quascirev.2006.07.012

Pedro, J.B., McConnell, J.R., van Ommen, T.D., Fink, D., Curran, M.A.J., Smith, A.M., Simon, K.J., Moy, A.D., Das, S.B., 2012. Solar and climate influences on ice core ^{10}Be records from Antarctica and Greenland during the neutron monitor era. Earth Planet. Sci. Lett. 355–356, 174–186. doi:10.1016/j.epsl.2012.08.038

Rach, O., Brauer, A., Wilkes, H., Sachse, D., 2014. Delayed hydrological response to Greenland cooling at the onset of the Younger Dryas in western Europe. Nat. Geosci. 7, 109–112. doi:10.1038/ngeo2053

Raisbeck, G.M., Yiou, F., Fruneau, M., Loiseaux, J.M., Lieuvin, M., Ravel, J.C., 1981. Cosmogenic ^{10}Be/^{7}Be as a probe for atmospheric transport processes. Geophys. Res. Lett. 8, 1015–1018. doi:10.1029/GL008i009p01015

Rasmussen, S.O., Andersen, K.K., Svensson, A.M., Steffensen, J.P., Vinther, B.M., Clausen, H.B., Siggaard-Andersen, M.L., Johnsen, S.J., Larsen, L.B., Dahl-Jensen, D., Bigler, M., Röthlisberger, R., Fischer, H., Goto-Azuma, K., Hansson, M.E., Ruth, U., 2006. A new Greenland ice core chronology for the last glacial termination. J. Geophys. Res. Atmos. 111, D06102. doi:10.1029/2005JD006079

Schuler, C., Wieland, E., Santschi, P.H., Sturm, M., Lueck, A., Bollhalder, S., Beer, J., Bonani, G., Hofmann, H.J., Suter, M., Wolfli, W., 1991. A multitracer study of radionuclides in Lake Zurich, Switzerland: 1. Comparison of atmospheric and sedimentary fluxes of ^{7}Be, ^{10}Be, ^{210}Pb, ^{210}Po and ^{137}Cs. J. Geophys. Res. 96, 17051–17065.

Siegenthaler, U., Heimann, M., Oeschger, H., 1980. ^{14}C variations caused by changes in the global carbon cycle. Radiocarbon 22, 177–191.

Snowball, I., Muscheler, R., 2007. Palaeomagnetic intensity data: an Achilles heel of solar activity reconstructions. The Holocene 17, 851–859. doi:10.1177/0959683607080531

Vogler, S., Jung, M., Mangini, A., 1996. Scavenging of ^{234}Th and ^{7}Be in Lake Constance. Limnol. Oceanogr. 41, 1384–1393.

Vonmoos, M., Beer, J., Muscheler, R., 2006. Large variations in Holocene solar activity: Constraints from ^{10}Be in the Greenland Ice Core Project ice core. J. Geophys. Res. 111, A10105. doi:10.1029/2005ja011500

Weltje, G.J., Tjallingii, R., 2008. Calibration of XRF core scanners for quantitative geochemical logging of sediment cores: Theory and application. Earth Planet. Sci. Lett. 274, 423–438. doi:10.1016/j.epsl.2008.07.054

Willenbring, J.K., von Blanckenburg, F., 2010. Meteoric cosmogenic Beryllium-10 adsorbed to river sediment and soil: Applications for Earth-surface dynamics. Earth-Science Rev. 98, 105–122. doi:10.1016/j.earscirev.2009.10.008

Zolitschka, B., 1998. A 14,000 year sediment yield record from western Germany based on annually laminated lake sediments. Geomorphology 22, 1–17. doi:10.1016/S0169-555X(97)00051-2

Table 1. Statistics for the linear regressions between the Meerfelder Maar $^{10}Be_{con}$ record and significantly correlated proxy time-series. **(a)** For simple linear regressions between $^{10}Be_{con}$ and SAR, Ti, Si/Ti ratio, TOC and Fe seperately. **(b)** For the multiple linear regression between $^{10}Be_{con}$ and all five significantly correlated proxy time-series. Only proxy time-series with a significant contribution (90 % level) were included in the final regression.

Fig. 1. Lake-catchment setting of Meerfelder Maar. Geographical position of Meerfelder Maar in western Europe. Topography of the Meerfelder Maar crater and bathymetry of the lake with location of composite sediment profile MFM09.

Fig. 2. Meerfelder Maar ^{10}Be concentrations ($^{10}Be_{con}$) and environmental proxy time-series from the same archive. $^{10}Be_{con}$ compared with sediment accumulation rate (SAR), Ti, Si/Ti ratio, total organic carbon (TOC) and Fe. The Laacher See Tephra was excluded from the analyses. Gray bars indicate $^{10}Be_{con}$ measurement uncertainties. Colored numbers indicate mean $^{10}Be_{con}$ for the early Holocene, Younger Dryas and late Allerød. Significance levels of correlations between $^{10}Be_{con}$ and proxy time-series were calculated using a random phase test (Ebisuzaki, 1997). Onset (12679 varve a BP) and termination (11590 varve a BP) of the Younger Dryas were defined from Meerfelder Maar sediments (Brauer et al., 2008; Martin-Puertas et al., 2012a).

Fig. 3. Correlation analyses of ^{10}Be concentrations ($^{10}Be_{con}$) and environmental proxy time-series from the investigated Meerfelder Maar sediments. $^{10}Be_{con}$ plotted against sediment accumulation rate (SAR), Ti, Si/Ti ratio, total organic carbon (TOC) and Fe. All datasets were normalized by dividing by the mean.

Fig. 4. Meerfelder Maar ^{10}Be concentrations ($^{10}Be_{con}$) corrected for the effects of varying environmental conditions. $^{10}Be_{con}$ corrected for changes in the environment ($^{10}Be_{atmosphere}$) as reflected by variations in sediment accumulation rates (SAR), Ti, Si/Ti ratio, total organic carbon (TOC) and Fe. The corrections were calculated using the individual environmental proxy time-series and all significantly correlated proxy time-series, to evaluate the largest possible environmental effects on $^{10}Be_{con}$ deposition (the final regression only includes the Si/Ti ratio and TOC proxies with a significant (90 % level) contribution). **(a)** $^{10}Be_{con}$ and calculated $^{10}Be_{atmosphere}$ time-series for the complete record from 11310 to 13130 varve a BP. **(b)** Same as **(a)**, but calculated separately for the early Holocene (11310-11570 varve a BP), Younger Dryas (11610-12670 varve a BP) and late Allerød (12690-13130 varve a BP). Before the analysis, all datasets were resampled to a 20-year resolution and normalized by dividing by the mean.

Fig. 5. 500-year high-pass filtered cosmogenic radionuclide records. The black line represents the Meerfelder Maar $^{10}Be_{atmosphere}$ composite (mean of the six $^{10}Be_{atmosphere}$ time-series for the period 11310 to 13130 varve a BP). Gray bands indicate the uncertainty ranges of the $^{10}Be_{atmosphere}$ composite expressed as the maximum differences between the individual $^{10}Be_{atmosphere}$ time-series. The red line depicts the reconstructed ^{14}C production rate (Muscheler et al., 2014). The blue line shows ^{10}Be flux in the GRIP ice core (Adolphi et al., 2014). The green line shows ^{10}Be flux in the GISP2 ice core (Finkel and Nishiizumi, 1997). Both ice core ^{10}Be records are on the GICC05 time-scale. The age of the Vedde Ash was determined to 12140 ± 40 varve a BP in the MFM2015 time-scale (Lane et al., 2013) and 12121 ± 114 a BP in the GICC05 time-scale of the GRIP/GISP2 ice cores (Rasmussen et al., 2006).

Fig. 6. Comparison of the Meerfelder Maar $^{10}Be_{atmosphere}$ composite with other cosmogenic radionuclide records. $^{10}Be_{atmosphere}$ composite and reconstructed ^{14}C production rate (Muscheler et al., 2014), ^{10}Be flux from the GRIP ice core (Adolphi et al., 2014) and ^{10}Be flux from the GISP2 ice core (Finkel and Nishiizumi, 1997) after high and bandpass filtering. Both ice core records are on the GICC05 time-scale. **(left)** 500-year high pass filtered time-series. **(middle)** Solar Gleissberg cycle (frequencies between 1/75 and 1/100 years^{-1}). **(right)** Solar De Vries cycle (frequencies between 1/180 and 1/230 years^{-1}). Gleissberg cycle variations cannot be investigated for the GISP2 ^{10}Be flux time-series due to the on average 50-year resolution of the record.

Table 1

(a) ^{10}Be corrected using single sig. proxy records
$^{10}Be_{atmosphere}$ (SAR)
$^{10}Be_{atmosphere}$ (Ti)
$^{10}Be_{atmosphere}$ (Si/Ti ratio)
$^{10}Be_{atmosphere}$ (TOC)
$^{10}Be_{atmosphere}$ (Fe)
(b) ^{10}Be corrected using all sig. proxy records
$^{10}Be_{atmosphere}$ (Si/Ti ratio + TOC; not significant at 90% level: SAR, Ti, Fe)

Figure 1
Click here to download high resolution image

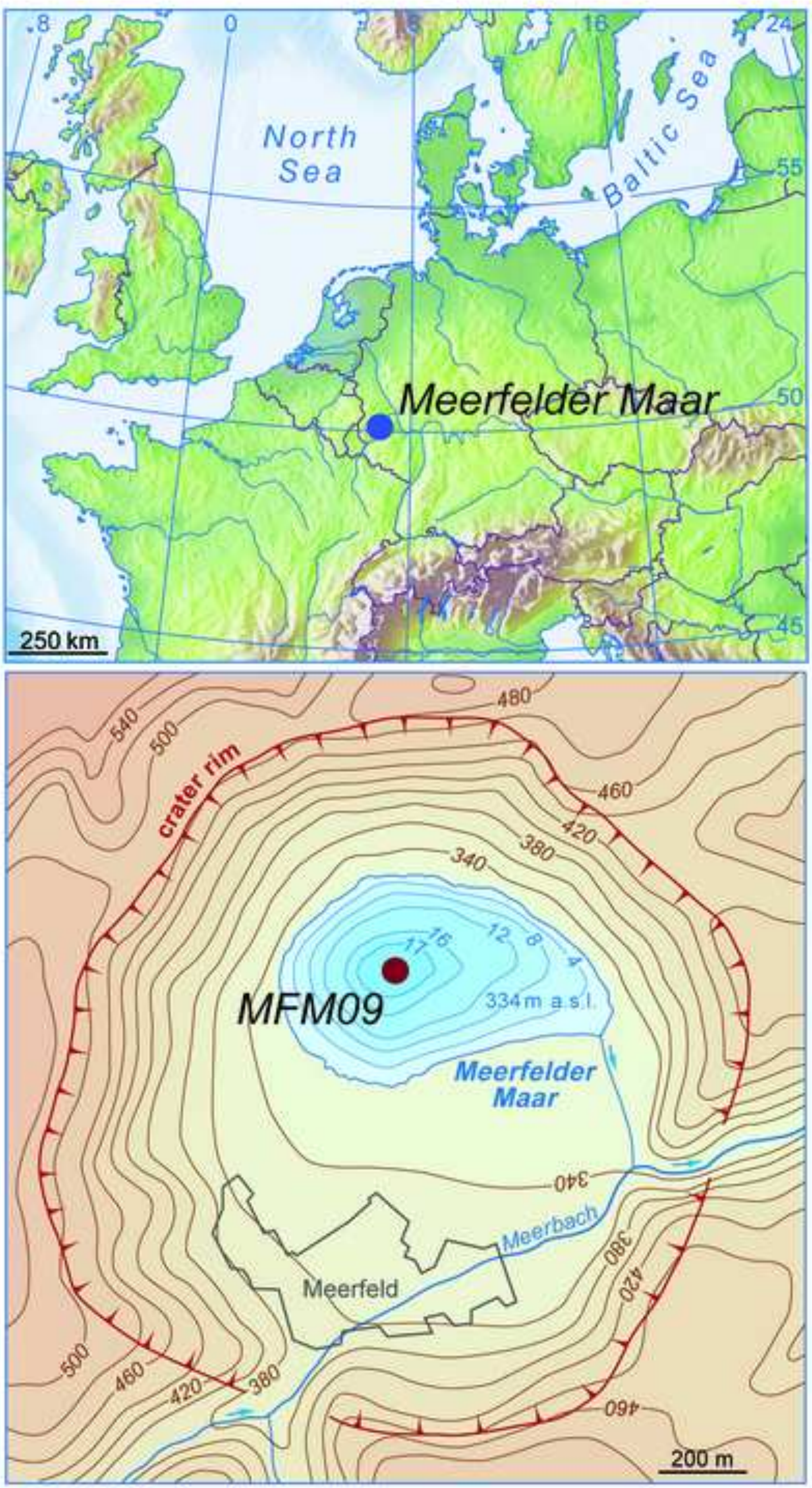

Figure 2

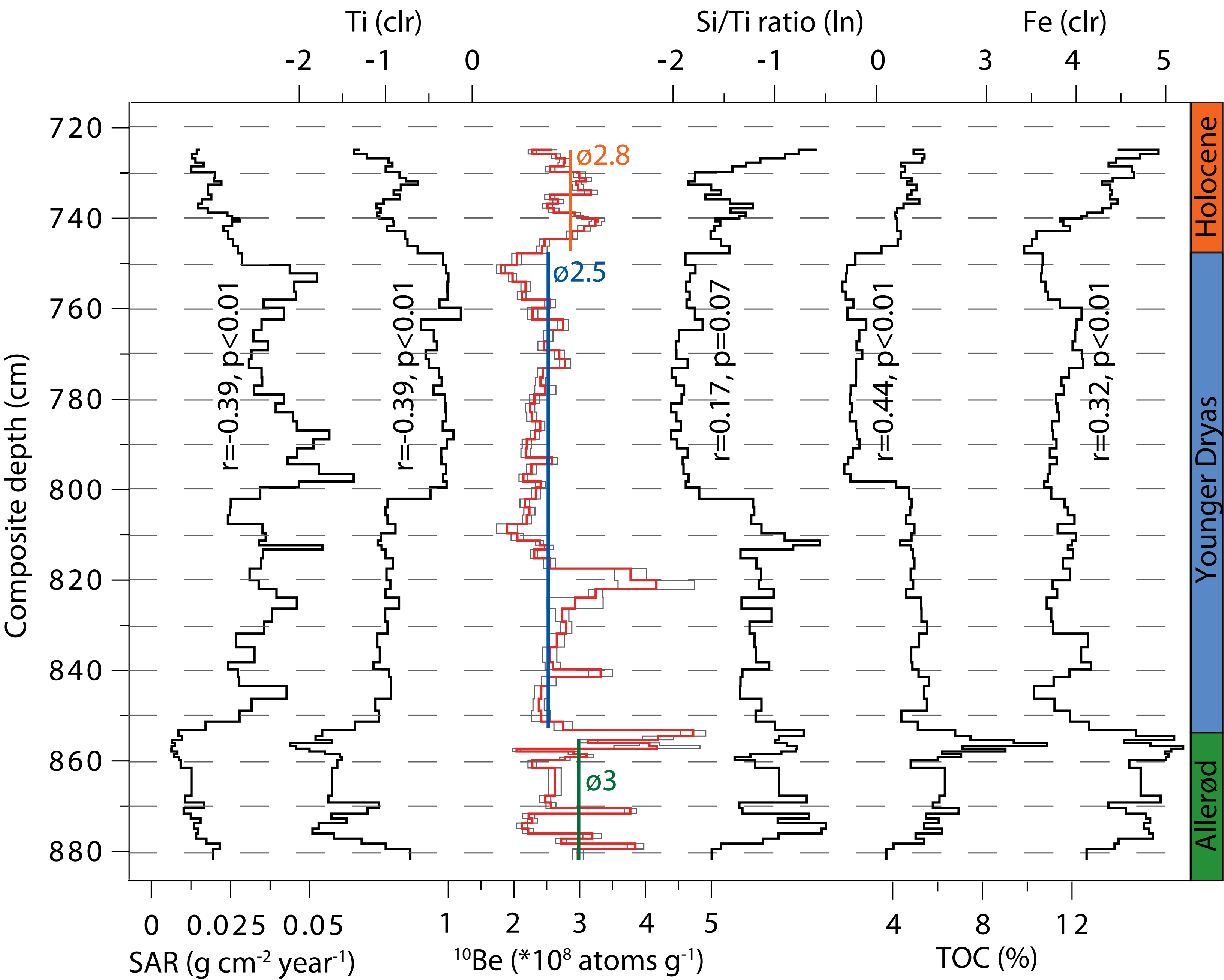

Ti (clr)
Si/Ti ratio (ln)
Fe (clr)
-2
-1
0
-2
-1
0
3
4
5
720
740
760
780
800
820
840
860
880
Composite depth (cm)
r=-0.39, p<0.01
r=-0.39, p<0.01
ø2.8
ø2.5
ø3
r=0.17, p=0.07
r=0.44, p<0.01
r=0.32, p<0.01
Holocene
Younger Dryas
Allerød
0
0.025
0.05
1
2
3
4
5
4
8
12
SAR (g cm-2 year-1)
10Be (*10^8 atoms g-1)
TOC (%)

Figure 3

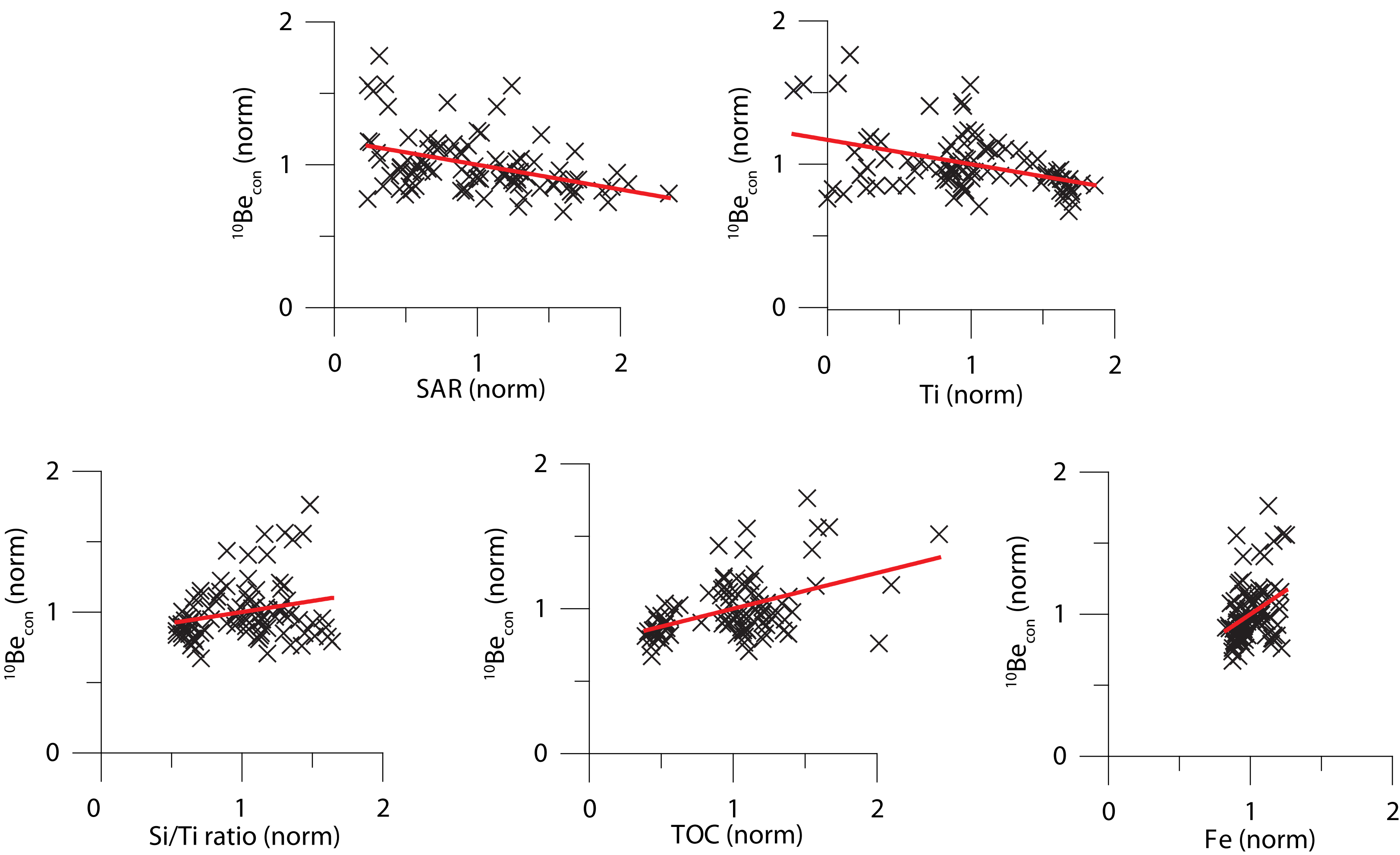

2
1
0
$^{10}Be_{con}$ (norm)
0
1
2
SAR (norm)
Ti (norm)
Si/Ti ratio (norm)
TOC (norm)
Fe (norm)

Figure 4

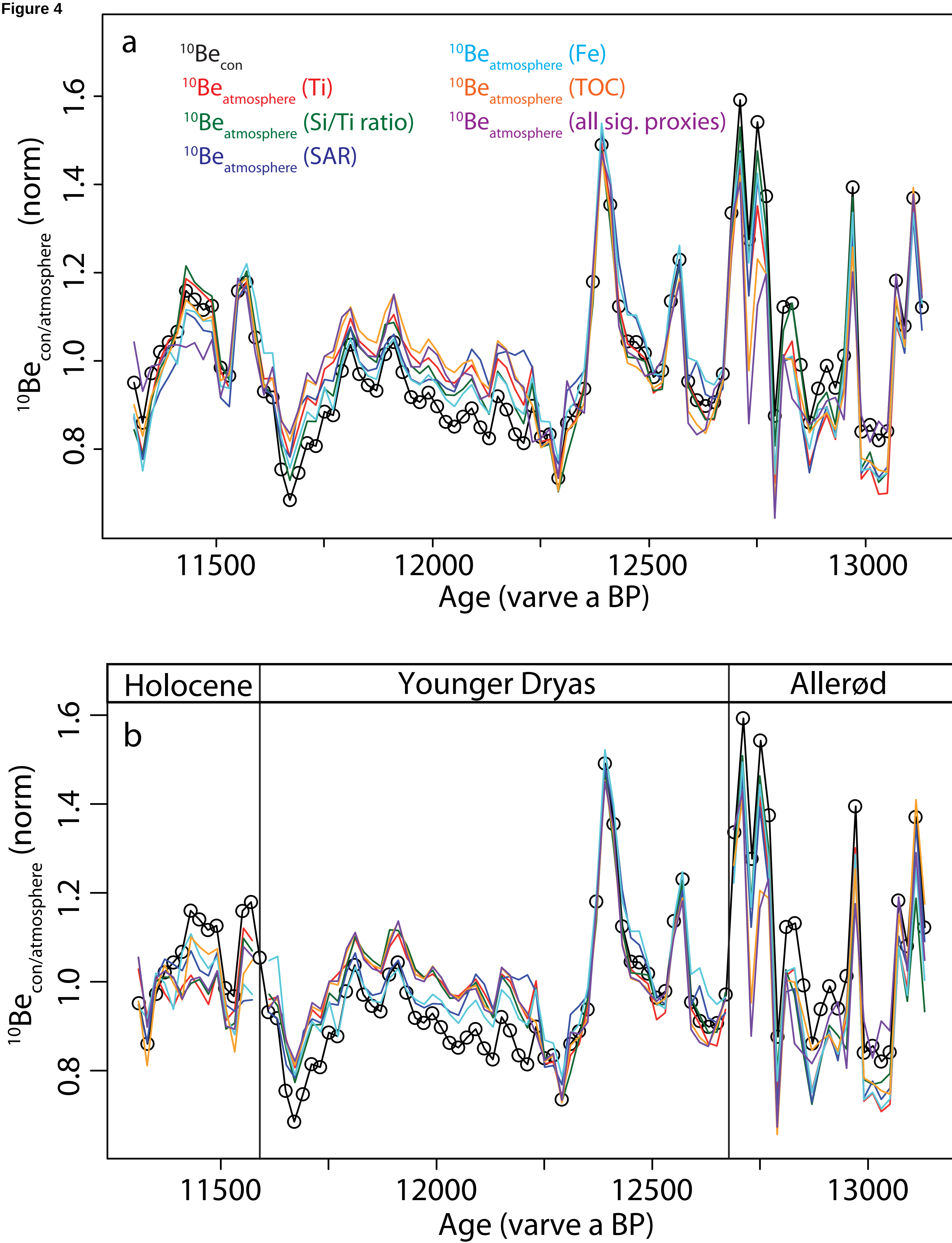

a
$^{10}Be_{con}$
$^{10}Be_{atmosphere}$ (Ti)
$^{10}Be_{atmosphere}$ (Si/Ti ratio)
$^{10}Be_{atmosphere}$ (SAR)
$^{10}Be_{atmosphere}$ (Fe)
$^{10}Be_{atmosphere}$ (TOC)
$^{10}Be_{atmosphere}$ (all sig. proxies)
$^{10}Be_{con/atmosphere}$ (norm)
0.8
1.0
1.2
1.4
1.6
11500
12000
12500
13000
Age (varve a BP)
Holocene
Younger Dryas
Allerød
b
$^{10}Be_{con/atmosphere}$ (norm)
0.8
1.0
1.2
1.4
1.6
11500
12000
12500
13000
Age (varve a BP)

Figure 5

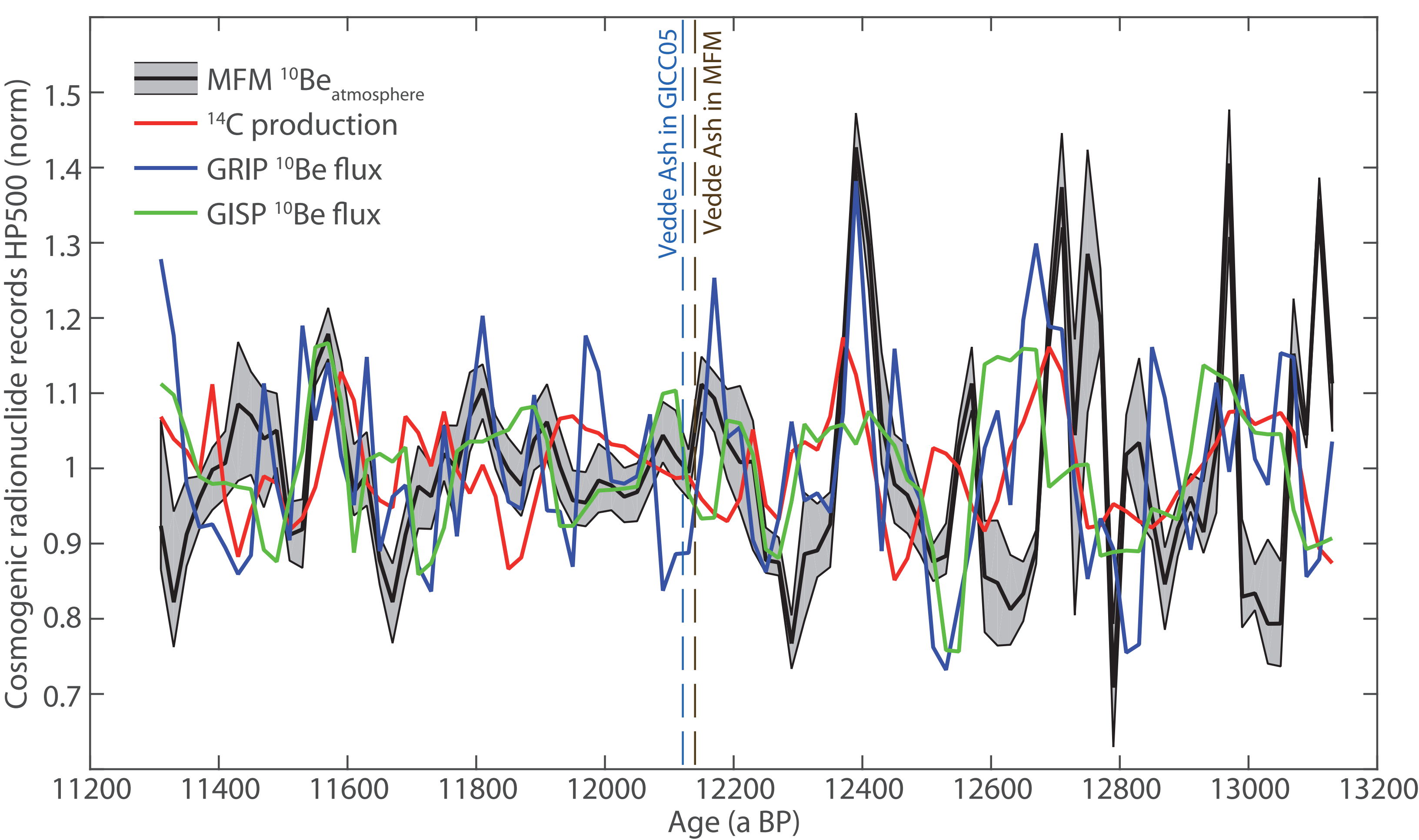

MFM $^{10}Be_{atmosphere}$
^{14}C production
GRIP ^{10}Be flux
GISP ^{10}Be flux
Vedde Ash in GICC05
Vedde Ash in MFM
Cosmogenic radionuclide records HP500 (norm)
1.5
1.4
1.3
1.2
1.1
1
0.9
0.8
0.7
11200
11400
11600
11800
12000
12200
12400
12600
12800
13000
13200
Age (a BP)

Figure 6

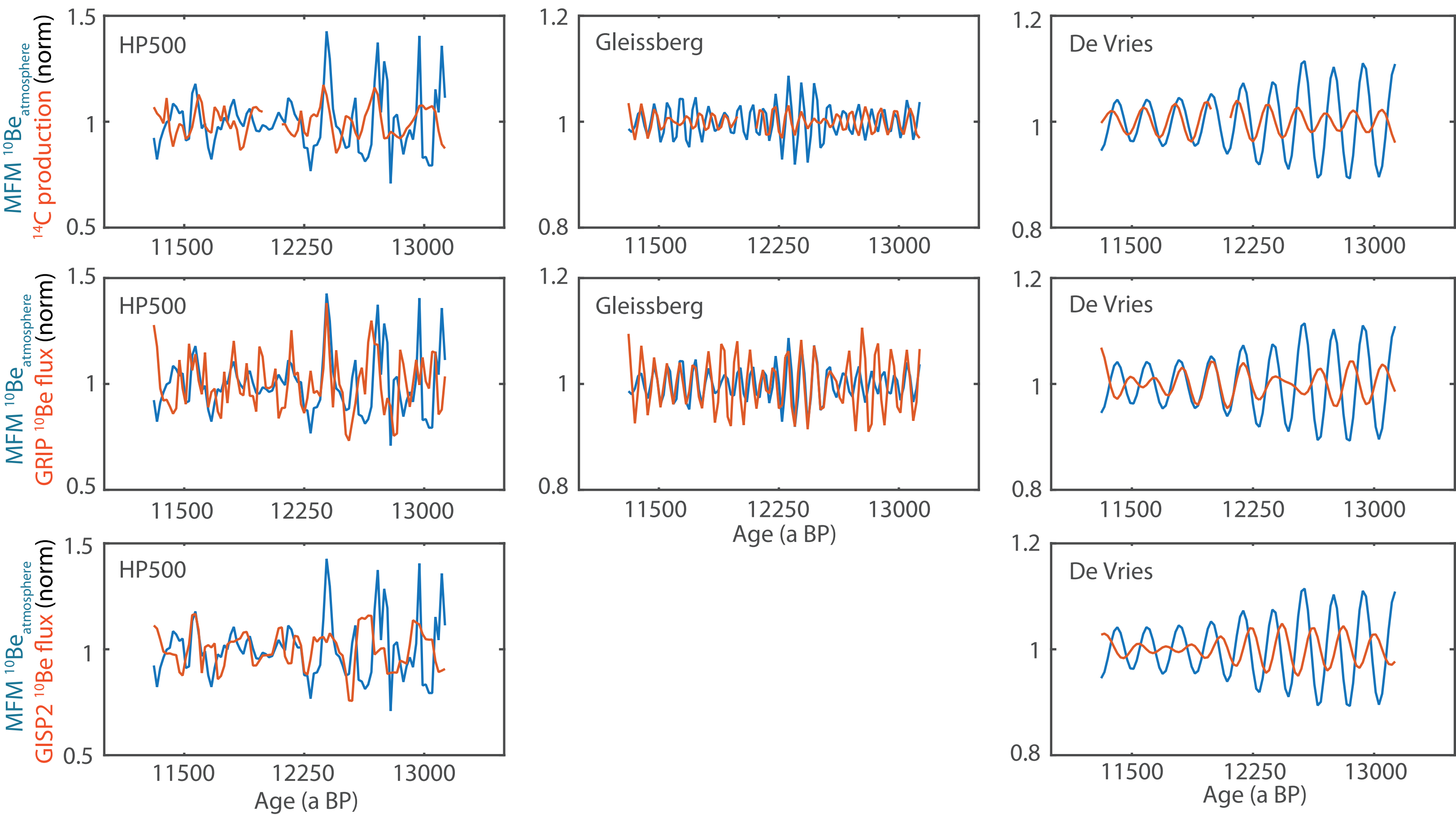
HP500
Gleissberg
De Vries
MFM ^{10}Be$_{atmosphere}$
^{14}C production (norm)
GRIP ^{10}Be flux (norm)
GISP2 ^{10}Be flux (norm)
1.5
1
0.5
1.2
0.8
11500
12250
13000
Age (a BP)

***Highlights (for review)**

Highlights:

^{10}Be record from varved lake sediments covering the Lateglacial-Holocene transition

New approach quantifies environmental influences on ^{10}Be deposition

Indicates potential of ^{10}Be in varved lake sediments for solar activity reconstruction

Indicates potential of ^{10}Be in varved lake sediments as synchronization tool

Response to the reviewer’s comments

We thank the reviewer for the constructive comments, which helped to further improve our manuscript.

Reviewer #2: The manuscript has been improved in response to my initial comments. I list several points below that still require some revisions. With these revisions addressed I think the manuscript is suitable for publication. I do not need to see the manuscript again.

1). The authors modified the title in response to my initial comments but maintain the claim in the abstract and conclusion that they are presenting a "record of solar activity variations". Records of solar activity are directly used (and sometimes misused) in forcing paleoclimate model runs. If they think their record is something that is suitable to be used as such a forcing then they might persist with this claim. Otherwise I would suggest to back it off as in the title or, at the very least, add some qualification on this point.

2). From the abstract line 35: "Our data suggest that environmental influences on the catchment do not substantially bias major 10Be excursions on multi-decadal scales, but contribute to up to 37 % of variability". This sentence does not make sense. The review response distinguished between correlation and 'multi-decadal 10Be excursions'. A couple of sentences are needed here to state the results of your regression analysis (environmental influences contribute up to 37% of the variance: r = 0.63 is not minor!) and separately state your point about also seeing major shifts in 10Be that are not mirrored by changes in these environmental variables. This two points are different and this must be explained clearly.

3) Abstract line 36: "The 10Be record dominantly reflects changes in solar activity". Given that the environment-corrected 10Be record is not quantitatively tested against other more established records of solar activity this statement should be qualified. e.g. "We interpret that the 10Be record dominantly reflects...". The same point applies in the Discussion and Conclusion.

4) Line 343: "(i) Increased sediment flux through the water column tends to increase 10Be scavenging and, thereby, does not distinctly influence 10Be concentrations in the sediments". This statement assumes that the available 10Be store in the water column is never a limiting factor. This may be the case, but please add a couple of sentences to acknowledge the assumption and explain why it is reasonable.

Minor point:
Line 65: Its not a case of 'might'; 10Be deposition *is* spatially variable.

We modified our manuscript according to the reviewer’s suggestions.

Appendix 1

Click here to download Supplementary Data: Czymzik et al. Appendix 1.xls